Numerical Study of Heat Transfer and Comfort Conditions in an Air-Cooled Ventilated Room with a Human Heat Source

Z. C. Briceño and J. F. Hinojosa*

Department of Chemical Engineering and Metallurgy, University of Sonora, CP 83000, Hermosillo, Sonora, Mexico

Abstract: A numerical study of the turbulent heat transfer in a two-dimensional rectangular air-cooled ventilated room with a human being as a discrete heat source was carried out in order to determine the best ventilation configuration. The results were obtained for a cavity of 2.5 m of height and 3.0 m of width. The right and left vertical walls of the cavity were kept at 35°C and 25°C respectively, whereas the remaining walls were adiabatic. Three cases for the air inlet and outlet locations were considered for the analysis. The air enters to the cavity at 15°C with speeds between 0.2 m/s and 2.0 m/s. The emissivity of the cavity walls was considered as 0, 0.5 and 1. The results indicate that the configuration (A) (inlet on the lower part of the right vertical wall and outlet on the upper part of the left vertical wall) offers the lowest average temperatures inside the room and the highest temperature distribution effectiveness.

Keywords: Turbulent heat transfer, ventilated room, discrete heat generation, radiative exchange.

1. INTRODUCTION

Buildings inhabited by people must provide them healthy and comfortable spaces to live and work, but these constructions also need to be energy efficient as possible in order to contribute to the maintenance of the environment. Due to the increase of energy consumption and greenhouse emissions, the energy consumption reduction for heating and cooling loads in buildings is an important task.

An important share of energy consumption comes from regions of the world with arid climate also known as desert climate. The above because buildings and houses need artificial air conditioning systems to achieve comfort conditions, which explain the high consumption of electricity. Thus to create a suitable environment in terms of air velocity and temperature with the minimum energy supply, the study of air movement and heat transfer in air-cooled ventilated rooms is an important aspect for the correct design of the ventilation systems.

In the specialized literature are reported several studies related with the airflow and heat transfer in ventilated cavities. Some of them will be briefly described next.

1.1. Air Flow and Heat Transfer in Ventilated Cavities without Discrete Heat Generation

Raji and Hasnaoui [1, 2] analyzed the mixed convection heat transfer in a two-dimensional ventilated cavity subjected to a uniform heat flux, considering different configurations. Flow patterns, temperature fields and heat transfer rates are examined for the following ranges of Rayleigh and Reynolds numbers: $10^3 \leq Ra \leq 5x10^6$ and $5 \leq Re \leq 5000$. The authors observed that the configuration with inlet and outlet at the bottom is the less useful for heat evacuation causing higher values of mean temperature, whereas that configuration with inlet at the bottom and outlet at the top was found to be more useful to reduce the mean temperatures inside the cavity for $Re \leq 1000$. Raji and Hasnaoui [3] evaluated the interaction between mixed convection and thermal radiation in a two-dimensional ventilated cavity with an aspect ratio of 2. Results showed that the radiation effect contributes to the homogenization of the temperature inside the cavity and to reduce the mean and maximum temperatures.

Singh and Sharif [4] conducted a numerical investigation of laminar mixed-convective cooling of a rectangular cavity with six different configurations to identify the optimum placement of inlet and exit for best cooling effectiveness. Their results showed that the configuration with the inlet on the lower side of the cold wall and the outlet on the upper side of the hot wall produces higher cooling efficiency, higher average Nusselt number at the hot wall and lower bulk average temperature. J. Posner [5], made a comparison of numerical studies with CFD and experimental results of a scaled room with laser Doppler anemometry (LDA) and particle laser velocimetry (PIV). The experimental test room was 91.4 x 45.7 x 30.5cm (scale 1:10) and the inlets were sized 10.1cm. The simulations showed that the RNG turbulence model is more accurate to predict the flow in a divided room and the relative errors were no greater than 20%.

*Address correspondence to this author at the Department of Chemical Engineering and Metallurgy, University of Sonora, CP 83000, Hermosillo, Sonora, Mexico; E-mail: fhinojosa@iq.uson.mx

E-ISSN: 2409-5826/16

Moraga and Lopez [6] performed a numerical analysis for a three-dimensional cooled cavity considering mixed convection. Near the hot wall, the fluid flow is always enclosed to the wall and has an ascendant direction that influences the air movement. Haslavsky *et al*. [7] carried out experiments to study the interactive phenomena in buoyancy-induced natural ventilation in a full scale enclosure with upper and lower openings on one of the sidewalls. Both the transient process and steady state interaction are explored. Experiments show that the mixing and displacement modes interact through a new combined ventilation model.

Rahman *et al*. [8] performed a numerical study of mixed convection in a square vented enclosure. They evaluated various inlet port configurations and the combined effect of various Prandtl, Reynolds and Richardson numbers. Streamlines, isotherms, average temperature and average Nusselt number at the heated wall are reported for a Ri from 0 to 10; Re=50, 100 and 200, and Pr=0.71, 7.5 and 50. From the results it is observed for low Ri, the Nusselt number reaches a minimum near the onset of flow separation along the heated wall, this behavior is not observed at high Pr and with the increase of Ri since no flow separation exists along the heated wall, the behavior is more linear. Daghigh, *et al*. [9], presented results of the air exchange rate (ACH) and air exchange effectiveness (AEE) on the thermal comfort of a naturally ventilated office. They tested the influences of 14 arrangements of window and door apertures indicating that the window and door arrangements significantly affect the air movement and thermal comfort.

Raji *et al*. [10] studied the heat transfer by mixed convection in a two-dimensional ventilated cavity. The numerical results show the flow structure is influenced by the interaction of the natural and forced convection. Saha, *et al*. [11], studied numerically free and forced convection in a rectangular cavity with a heat source at the bottom and air inlet and outlet at the sides. Three Reynolds numbers were chosen (Re=50, 100 and 200) and Richardson number from 0 to 10. The results showed that the heat transfer coefficient is strongly affected by Re and Ri numbers, also an empirical correlation was developed with Nusselt, Reynolds and Richardson numbers.

Tanny *et al*. [12] studied experimentally the effect of the ventilation on the airflow characteristics through the upper vent of a naturally ventilated full-scale enclosure, presenting velocity vectors, turbulence of the flow as well as temperature profiles and heat fluxes. Lariani *et al*. [13] reported results of air velocity and temperatures on a ventilated cavity where an air jet enters at 16°C. Experimental measurements and numerical predictions were obtained. The results show that the temperature distribution is three-dimensional and an elevated vertical gradient from the floor exists.

Xamán *et al*. [14] studied numerically the heat transfer in a ventilated cavity. Four cases for the air outlet location were considered in the analysis; The incoming air velocity was varied by changing the Reynolds number between $2x10^3 \leq Re \leq 4x10^4$. Two different materials were tested for the conductive wall (construction brick and adobe block) and three different widths each (0.1, 0.2 and 0.3 m). From the results can be concluded that the 0.3 m width adobe block is the appropriate to minimize thermal load gains and that the right side of the upper horizontal wall was the best position for the air exhaust based on the effectiveness of temperature distribution.

Rodriguez and Hinojosa [15] presented three-dimensional numerical results in a ventilated room considering three different inlet configurations. The study was carried out considering turbulent flow and the radiative exchange between the walls. The air inlet velocity was 0.5 m/s and the emissivity of the walls was considered as 0.8. The temperature fields, flow patterns, heat transfer coefficients and temperature distribution effectiveness are presented and discussed. It was found that the results obtained without the consideration of the thermal radiation provide underestimated values for the average temperature and the local temperatures inside the room, which affect the decisions concerning the dimensioning and use of air conditioning systems.

1.2. Air Flow and Heat Transfer in Ventilated Cavities with Discrete Heat Generation

Papanicolaou and Jaluria [16] carried out a numerical study of the mixed convection in a rectangular ventilated cavity with a discrete heat source in it. The effects of the Reynolds number, Richardson number, position of the heat source and position of the outflow on heat transfer and temperature distribution were observed for a Reynolds number from 50 to 2000. The obtained results were used to study heat removal mechanisms in practical systems. In another study, these authors [17] studied numerically a problem of mixed convection considering a cavity with two

ventilation ports, conductive walls and a discrete heat source on a wall. The Reynolds number was fixed at 100 and Richardson number was varying between 0-10. The results show that the configuration in which the two types of convection are assisted presents higher heat transfer and lower sources temperatures.

Hsu and Wang [18] performed a numerical study about mixed convection in a ventilated cavity with discrete heat sources embedded on a vertical board which is situated on the bottom wall of the enclosure. The Reynolds number was studied from 100 to 1000. They found that when the source is located on the right surface of the board the Nusselt number is not depending neither on the variation of the location of the source nor of the board. Radhakrishnan *et al*. [19] reported a numerical and experimental work about turbulent mixed convection in a ventilated cavity with adiabatic walls and a discrete heat source inside. Correlations were developed for the average Nusselt number and the maximum dimensionless temperature occurring in the heat source, in these parameter ranges: 1200≤Re≤10000 and 0.003≤Ri≤0.2. The authors concluded that a combined experimental and numerical investigation would significantly reduce the effort required to optimize the thermal performance in problems on this class.

Ghasemi and Aminossadati [20] studied numerically mixed convection in a two-dimensional ventilated cavity with discrete heat sources, examining the effects of the number and position of the sources, the Rayleigh number from 0 to 10^7 at a fixed Reynolds of 100. Results show that increasing significantly Rayleigh number improves the heat transfer process in the cavity. The arrangement of sources also has a great contribution on the cooling performance but when the Rayleigh number is increased this contribution decreases. Bilgen and Muftuoglu [21] investigated a cooling strategy in a square cavity with adiabatic walls and a heat source on the left wall. The Rayleigh number was studied from 10^3 to 10^7 and the Reynolds number from 10^2 to 10^3. The authors observed that optimal position of the source is almost insensitive to variation in Rayleigh and Reynolds numbers, but it is strongly affected by the arrangements on the ventilation ports. It was found that the highest cooling performance is given by placing the air outlet on the upper left part of the cavity.

According to the literature review, there are no reported numerical studies on ventilated cavities with a human being as a discrete heat source, and considering the combined effect of turbulent natural and forced convection with thermal radiation. Therefore, it is necessary to extend the knowledge on ventilated cavities with a human being inside and to analyze the appropriate thermal comfort aspects.

This work is focused to carry out a numerical analysis of comfort conditions and heat transfer by natural and forced convection with thermal radiation in an air-cooled ventilated two-dimensional cavity with turbulent flow and a human heat source. The numerical results were obtained considering velocities between 0.2 m/s and 2.0 m/s and the emissivity of the walls as 0, 0.5 and 1; in addition, three different configurations for the air inlet and outlet location were considered. The flow patterns, temperature fields, average temperatures, the temperature distribution effectiveness and the dimensionless heat transfer parameters are presented and discussed.

2. PHYSICAL AND MATHEMATICAL MODEL

2.1. Physical Model

The study of the air movement and the heat transfer by combined convection (natural and forced) and

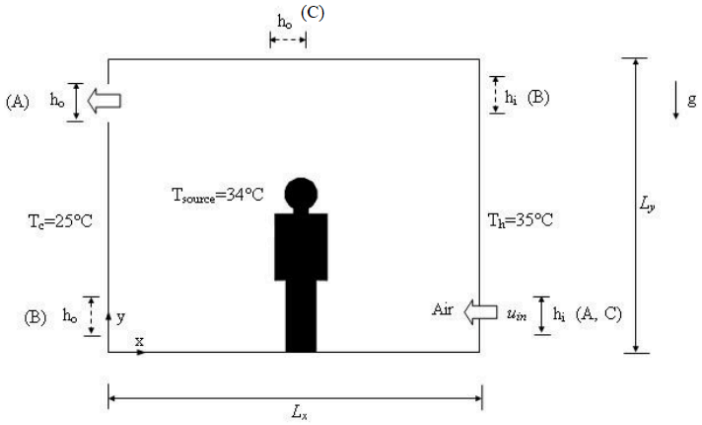

Figure 1: Physical model of the ventilated cavity with a human being as a discrete heat source.

thermal radiation was carried out in a two-dimensional ventilated cavity (Figure **1**). The width of the cavity is 3m and the height is 2.5m. The left and the right vertical walls were assumed as isothermal at T_c (25°C) and T_h (35°C) respectively, whereas the horizontal walls were considered as adiabatic. The dimensions of the openings (inlets and outlets) were l_i=l_o=0.2m. The three different configurations of inlet and outlet positions are shown in Table **1**. The air enters to the cavity at 15°C, which is typical of air-conditioning ventilation systems, with speeds between 0.2m/s and 2.0m/s. Due to the size of the system being considered in this study, it is assumed that the flow regime of the fluid (air) in the system is turbulent. The air is not involved in radiative heat transfer therefore radiative exchange is between the walls of the cavity and the heat source. The height of the discrete heat source (human being) was 1.7m, whereas its temperature and emissivity were 34°C and 0.97 (human skin) respectively [22].

Table 1: Inlet and Outlet Positions

Configuration	Inlet (x, y)	Outlet (x, y)
A	(x=3.0, 0.2≤y≤0.4)	(x=0.0, 2.1≤y≤2.3)
B	(x=3.0, 2.1≤y≤2.3)	(x=0.0, 0.2≤y≤0.4)
C	(x=3.0, 0.2≤y≤0.4)	(1.4≤y≤1.6, y=2.5)

2.2. Mathematical Model

The steady state governing equations (mass conservation, momentum and energy) in time averaged tensor notation are as follow:

Continuity:

$$\frac{\partial \rho \overline{u_i}}{\partial x_i} = 0 \tag{1}$$

Momentum:

$$\rho \overline{u_j} \frac{\partial \overline{u_i}}{\partial x_j} = \frac{\partial \overline{P}}{\partial x_i} + \frac{\partial}{\partial x_j}\left[\mu \frac{\partial \overline{u_i}}{\partial x_j} - \rho \overline{u_i' u_j'} \right] + \rho g_i \tag{2}$$

Energy:

$$\rho \overline{u_j} \frac{\partial \overline{T}}{\partial x_j} = \frac{1}{C_p} \frac{\partial}{\partial x_j}\left[\lambda \frac{\partial \overline{T}}{\partial x_j} - \rho C_P \overline{T' u_j'} \right] \tag{3}$$

where x_i and x_j are the Cartesian coordinates of the system (i=x,y and j=x,y), $\overline{u}$ is the mean velocity, $\overline{P}$ is the mean dynamic pressure, $\overline{T}$ is the mean temperature, g is the gravitational acceleration. ρ, Cp, λ are the density, the specific heat at constant pressure and the thermal conductivity of the fluid respectively.

In the family of eddy viscosity models (EVM), the Reynolds stress tensor is established through the Boussinesq hypothesis as:

$$\rho \overline{u_i' u_j'} = -\mu_t \left(\frac{\partial \overline{u_i}}{\partial x_j} + \frac{\partial \overline{u}_j}{\partial x_i} \right) + \frac{2}{3} \rho k \delta_{ij} \tag{4}$$

The model of high Reynolds number (HRN) considers that the turbulent viscosity (μ_t) is given by:

$$\mu_t = \rho C_\mu \frac{k_t^2}{\varepsilon_t} \tag{5}$$

where C_μ is a constant.

The turbulent heat fluxes are expressed as:

$$\rho C_P \overline{T' u_i'} = -\frac{\mu_t}{\sigma_T} \left[\frac{\partial \overline{T}}{\partial x_i} \right] \tag{6}$$

where σ_T is the turbulent Prandtl number.

The turbulent kinetic energy (k_t) and the dissipation of the turbulent kinetic energy (ε_t) are obtained with the turbulence model of Ince and Launder [23]:

Turbulent kinetic energy (k_t):

$$\frac{\partial (\rho \overline{u}_i k_t)}{\partial x_i} = \frac{\partial}{\partial x_i}\left[\left(\mu + \frac{\mu_t}{\sigma_{k_t}} \right) \frac{\partial k_t}{\partial x_i} \right] + P_{kt} + G_{kt} - \rho \varepsilon_t \tag{7}$$

Dissipation of the turbulent kinetic energy (ε_t):

$$\frac{\partial (\rho \overline{u}_i \varepsilon_t)}{\partial x_i} = \frac{\partial}{\partial x_i}\left[\left(\mu + \frac{\mu_t}{\sigma_{\varepsilon_t}} \right) \frac{\partial \varepsilon}{\partial x_i} \right] + C_{1\varepsilon} \frac{\varepsilon_t}{k} \left[P_{k_t} + C_{3\varepsilon_t} G_{k_t} \right] - C_{2\varepsilon} \rho \frac{\varepsilon_t^{\,2}}{k_t} \tag{8}$$

where:

$$P_{kt} = -\mu_t \left[2\left(\frac{\partial \overline{u_i}}{\partial x_i} \right)^2 + \left(\frac{\partial \overline{u_i}}{\partial x_j} \right)^2 \right] \tag{9}$$

$$G_{k_t} = -\beta g_i \frac{\mu_t}{\sigma_T} \frac{\partial \overline{T}}{\partial x_i} \tag{10}$$

In above equations the terms $C_{1\varepsilon}$ and $C_{2\varepsilon}$ are coefficients; whereas σ_k and σ_ε are the turbulent Prandtl numbers.

The radiation heat transfer occurs through radiative exchange among the walls and the heat source of the cavity. For an opaque surface, the leaving intensity (also called radiosity) is composed of the emitted intensity and the reflected irradiation:

$$I = \varepsilon I_b + \frac{\rho}{\pi}\int_{2\pi} I'(\hat{s}_i)\Phi(\hat{s}_i,\hat{s})d\Phi_i \tag{11}$$

where ε and ρ are the emissivity and reflectivity respectively, I_b is the blackbody intensity, Ω_i is the solid angle, is $\hat{s}$ the propagation direction, I is the leaving intensity and I′ is the incoming intensity. The net radiant heat flux of a surface is the difference between the radiosity and irradiation:

$$q_r = \int_{2\pi} I\Phi(\hat{s}_i,\hat{s})d\Phi_i - \int_{2\pi} I'(\hat{s}_i)\Phi(\hat{s}_i,\hat{s})d\Phi_i \tag{12}$$

In order to obtain the hydrodynamic boundary conditions, the velocity components are equal to zero on the walls because the non-slip condition. The air was considered to enter perpendicular to the opening; therefore, the x-component of the velocity had a constant value whereas the y-component is equal to zero. For the outlets, a fully developed flow was assumed. The turbulent kinetic energy and the dissipation of the turbulent kinetic energy for the incoming air were obtained by applying the empirical correlations reported by Nielsen [24]:

$$k_{in} = 1.5\left(0.04U_{in}\right)^2 \tag{13}$$

$$\varepsilon_{in} = \frac{\left(k_{in}\right)^{0.5}}{L_{in}} * 0.1 \tag{14}$$

The thermal boundary conditions are as follows:

$$T(3.0,0\le y<2.1\cup 2.3<y\le 2.5)=T_h \tag{15}$$

$$T(0,0\le y<0.2\cup 0.4<y\le 2.5)=T_c \tag{16}$$

$$\left.\frac{\partial T}{\partial y}\right|_{0\le x\le 3, y=0} = q_{r1} \tag{17}$$

$$\left.\frac{\partial T}{\partial y}\right|_{0\le x\le 3, y=2.5} = q_{r2} \tag{18}$$

$$T_{in} = 288\ K \tag{19}$$

where q_{r1} and q_{r2} are the net radiative heat fluxes of the corresponding adiabatic surface.

With the purpose of generalizing the results, the non-dimensional Reynolds (Re) and Rayleigh (Ra) numbers, were defined as follows:

$$Ra = \frac{g\beta\left(T_h - T_c\right)L_y^{\ 3}}{\nu\alpha} \tag{20}$$

$$\mathrm{Re} = \frac{u_{in}h_i}{\nu} \tag{21}$$

where g is the gravity, v is the kinematic viscosity, L_y is the height of the cavity, h_i is the height of the air inlet, u_{in} is the inlet velocity, α and υ are the thermal diffusivity and the kinematic viscosity of the fluid respectively.

The local convective and radiative Nusselt numbers were defined as:

$$Nu_c = \frac{q_{convection}}{q_{conduction}} = \frac{h\,L_{ref}}{\lambda} \tag{22}$$

$$Nu_r = \frac{q_{radiation}}{q_{conduction}} = \frac{q_r}{\lambda\left(T_h - T_{ref}\right)/L_{ref}} \tag{23}$$

where h is the local convective heat transfer coefficient, q_r is the local radiative heat flux of the wall, T_{ref} is the temperature of incoming air (T_{in}) and L_{ref} is the value of L_x. The average convective Nusselt number ($\overline{Nu_c}$) and the average radiative Nusselt number ($\overline{Nu_r}$) were obtained by integrating the local Nusselt numbers over the surface.

The global temperature distribution effectiveness indicates the way in which temperature pattern is distributed along the room. It is defined as [25]:

$$\overline{\varepsilon}_T = \frac{T_{out} - T_{in}}{T_{mean} - T_{in}} \tag{24}$$

where T_{out} is the air average temperature at the outlets, T_{mean} is the air average temperature inside the room and T_{in} is the air average temperature at the inlet.

3. NUMERICAL METHOD

The CFD software Fluent 6.3 was used to obtain the numerical results, which is based on the finite volume method to solve the governing equations of the fluid motion and heat transfer. The algorithm SIMPLE was considered to couple the momentum and continuity equations. Convective terms were discretized applying the Power Law scheme given by Patankar [26]. The

radiative heat transfer model was solved with the discrete ordinate method. In this method the radiative heat transfer equations with their respective boundary conditions are solved for a set of different directions assuming that the intensity remains constant within the control volume and the integrals are approximated using a Gaussian quadrature over all the solid angle.

The convergence criterion was 10^{-3} for the residual of each equation. The independence mesh analysis was carried out considering a velocity inlet of 2.0m/s and ε=1.0. Different mesh sizes starting with 100x80 until 160x140 with an increment of 10x10 nodes. It was found that the average total Nusselt number of the hot wall was independent of the mesh size for a mesh size of 150x130 nodes (26537 nodes). The solid angle divisions for the discrete ordinate method was varied and was found that the total average Nusselt number of the hot wall remains constant with 32 discrete angles.

In order to validate the numerical code, a comparison against the experimental results reported by Nielsen [24] and Radhakrishnan *et al*. [19] was made. The experimental results of Nielsen correspond to an isothermal ventilated cavity with the following dimensions: 3.0m x 3.0m x 9.0m. The air enters through an aperture located in the upper side of the left wall and leaves the cavity by an aperture on the lower side of the right wall. Figure **2** shows a good agreement between the numerical and experimental velocity profiles. However, the experimental results of Radhakrishnan *et al*. were obtained in a ventilated cavity with a heat source. The heat power of the heat source was fixed at 10.1 W. The percentage differences between numerical and experimental Nusselt numbers are presented in Table **2**; the maximum and minimum absolute differences were 9.55% (Re=9000) and 2.09% (Re=7000) respectively.

Table 2: Comparison with Radhakrishnan *et al*. (2007)

Re	Nusselt number of this work	Nusselt number of Radhakrishnan *et al*. (2007)	%
3000	21.5	22.8	5.72
5000	31.3	30.0	4.35
7000	36.4	37.2	2.09
9000	37.8	41.8	9.55

4. RESULTS AND DISCUSSION

Next, the numerical results for three configurations of inlet/outlet ventilation are presented. Five values for the incoming air velocity were chosen: 0.2, 0.5, 1.0, 1.5 and 2.0m/s, corresponding to the following Reynolds numbers: $2.7x10^3$, $6.7x10^3$, $1.3x10^4$, $2.0x10^4$ and $2.7x10^4$. Three different values of the walls emissivity (ε) were analyzed: 0, 0.5 and 1. The Rayleigh number was fixed at $1.5x10^7$.

Figure **3** shows the flow patterns (streamlines) in the ventilated cavity considering an air inlet speed of 1m/s and an emissivity of the walls of 0.5. It is noted that the configuration affect the flow pattern inside the cavity. In configuration (A) the fluid enters by the bottom of the right wall, collides with the heat source, rises along it and goes out in the top of the left wall. Besides are observed: two large vortexes in the left section of the cavity rotating in opposite directions (the lower rotating clockwise), two vortexes above and

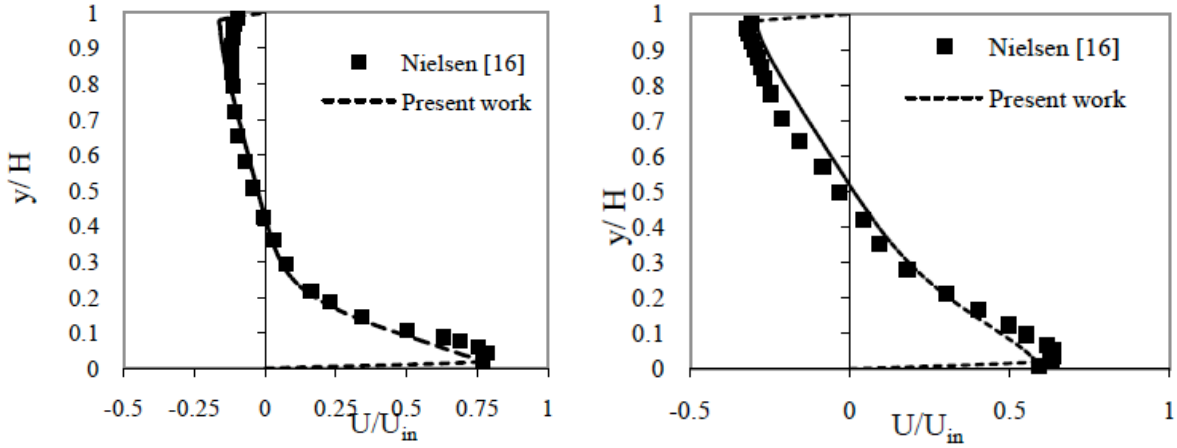

Figure 2: Comparison of velocity profiles from the present work and from Nielsen [14] at x=3m (**a**) and x=6m (**b**).

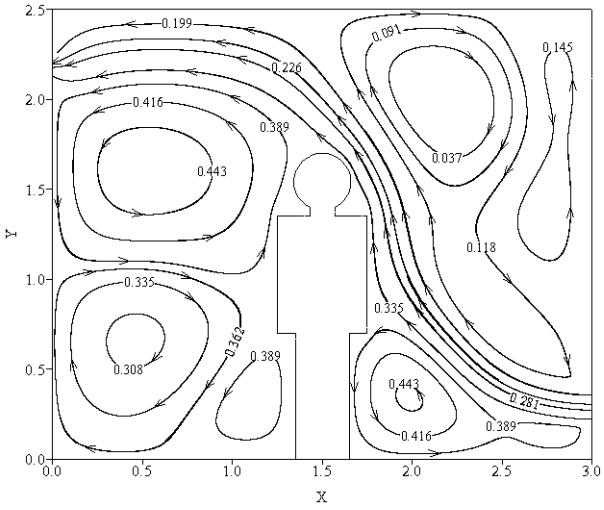

Configuration (A)

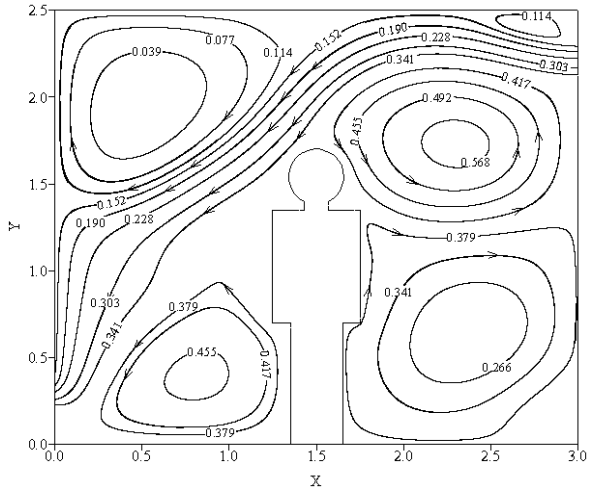

Configuration (B)

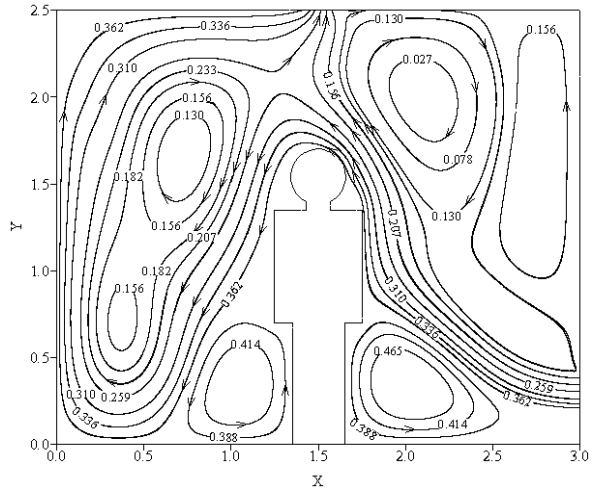

Configuration (C)

Figure 3: Streamlines (flow patterns) in the ventilated cavity for Re=6.7x10^3 and ε=0.5.

below the main flow stream in the right section of the cavity and smaller vortexes adjacent to the legs of the source. In configuration (B) the air enters the cavity through the top of the right wall and displaces near the roof, until at half, it drops to exit through the bottom of the left wall. In the left section of the cavity two large vortexes are formed, one above the main stream of fluid (with clockwise rotation) and one below (with counterclockwise rotation), while in the right section two big vortexes are observed rotating with opposite direction (the upper vortex rotates clockwise) and a small vortex in the upper right corner of the cavity.

For configuration (C) the fluid enters through the bottom of the right wall, collides with the heat source and a part of it exits the cavity through the central region of the ceiling. The other part descends toward the left side and ascend impelled by the effect of natural convection (due to the temperature of the left wall is greater than the fluid) and finally leaves the cavity. In the lower region near the source is formed a clockwise recirculation, and on the right side of the cavity are formed two large vortexes above the main stream (the closer to the right wall rotates counterclockwise), and a smaller one at the bottom of the main current that rotates counterclockwise.

Figure **4** shows the temperature fields. It can be seen near the right wall the presence of higher temperature gradients. In configurations (A) and (C), the region of the right side of the cavity is the one with the lower temperatures while higher temperatures are presented in the left side, in the configuration (B), the opposite occurs because the fluid entering through the top of the right wall reduces the temperature of the left side of the cavity. Furthermore, for this inlet speed the configuration (C) is the one that better distributes the temperature inside the cavity, although the configuration (A) shows a larger area with lower temperatures (17-19°C).

The total average Nusselt numbers of the heated wall and the heat source (human) for the three configurations are presented in Tables **3-5**. It is observed in the three different configurations that the average total Nusselt number of the heated wall and heat source increase substantially with the Reynolds number (inlet velocity) and the emissivity of the walls. However for configuration (A) when the Reynolds number varies from 2.7x10^3 to 2.7x10^4, the average total Nusselt number of the heated wall increases between 94.5% (ε=1) and 103.5% (ε=0.5), whereas the average total Nusselt number of the heat source

increases among 155.7% (ε=1) and 225% (ε=0). For case (B) the same increase of Reynolds number causes that average total Nusselt number of the heat source increases among 84.0% (ε=1) and 93.0% (ε=0.5), whilst the average total Nusselt number of the heated wall raises between 72.7% (ε=0.5) and 76.2% (ε=1).

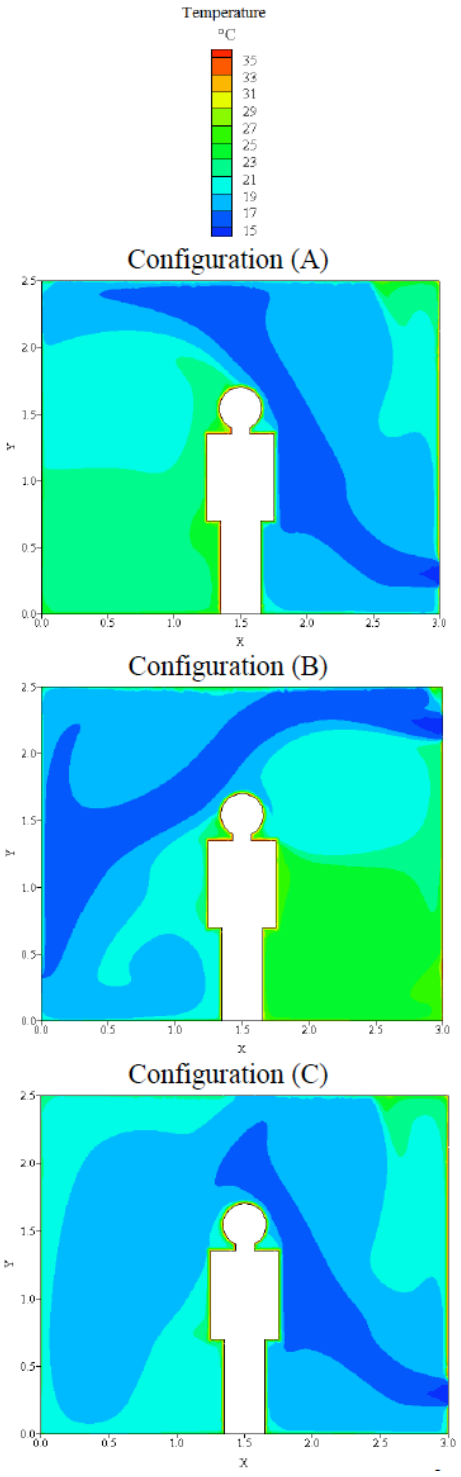

Figure 4: Temperature fields (°C) for Re=6.7x10^3 and ε=0.5.

Table 3: Average total Nusselt numbers for configuration (A)

Re	ε=0		ε=0.5		ε=1	
	Heated Wall	Human	Heated Wall	Human	Heated Wall	Human
2.7x10^3	689.7	462.1	738.2	666.0	919.4	760.1
6.7x10^3	742.5	568.8	861.8	900.8	1042.0	921.6
1.3x10^4	824.8	837.6	939.1	982.8	1164.5	1228.7
2.0x10^4	1051.9	1178.1	1277.5	1595.5	1415.2	1599.1
2.7x10^4	1378.0	1502.0	1503.0	1903.1	1788.3	1943.7

Table 4: Average Total Nusselt Numbers for Configuration (B)

Re	ε=0		ε=0.5		ε=1	
	Heated Wall	Human	Heated Wall	Human	Heated Wall	Human
2.7x10^3	531.96	448.66	630.05	622.43	749.37	687.44
6.7x10^3	538.86	476.18	659.69	824.74	824.20	881.22
1.3x10^4	639.06	612.71	814.52	925.36	965.21	984.25
2.0x10^4	748.82	770.12	924.09	1064.42	1139.60	1125.19
2.7x10^4	922.29	840.04	1088.01	1201.30	1320.19	1264.82

Table 5: Average Total Nusselt Numbers for Configuration (C)

Re	ε=0		ε=0.5		ε=1	
	Heated Wall	Human	Heated Wall	Human	Heated Wall	Human
2.7x10^3	696.7	462.6	780.4	654.8	948.1	792.2
6.7x10^3	734.1	571.7	874.3	879.4	1041.1	930.8
1.3x10^4	743.6	759.4	976.1	1012.8	1138.9	1125.4
2.0x10^4	1037.0	1042.9	1082.9	1162.7	1357.7	1408.9
2.7x10^4	1402.7	1375.3	1524.8	1713.8	1777.1	1759.3

Finally for configuration (C) the same rise of the Reynolds produces increases between 87.4% (ε=1.0) and 101.3% (ε=1) in the average total Nusselt number of the heated wall, while that the average total Nusselt number of the heat source increases within 122.1% (ε=1) and 197.3% (ε=0). Therefore, the effect of Reynolds number increase is more relevant in configurations (A) and (C).

On the other hand when the emissivity of the walls increases from 0 to 1, Configuration (A) leads to an increase of the average total Nusselt number of the heat source within 29.4% ($Re=2.7x10^4$) and 64.5% ($Re=2.7x10^3$), whereas the average total Nusselt number of the heated wall rises between 29.8% ($Re=2.7x10^4$) and 41.2% ($Re=1.3x10^4$). For configuration (B), the average total Nusselt number of the heated wall increase between 40.9% ($Re=2.7x10^3$) and 53.0% ($Re=6.7x10^3$), with the increase of the emissivity. While, the average total Nusselt number of the heat source increases within 46.1% ($Re=2.0x10^4$) and 85.1% ($Re=6.7x10^3$). For configuration (C) the average total Nusselt number of the heat source increases between 27.9% ($Re=2.7x10^4$) and 71.3% ($Re=2.7x10^3$), whilst the average total Nusselt number of the heated wall increases among 26.7% ($Re=2.7x10^4$) and 53.2% ($Re=1.3x10^4$). Hence, the increase of the emissivity of the walls is more important for configuration (B).

The comparison of total average Nusselt number for the three configurations, indicates that for all cases the values of configurations (A) and (C) are greater than configuration (B). The percentage differences of average Nusselt numbers of the heated wall between configurations (A) and (B) are within 13.3% ($Re=1.3x10^4$ and $\varepsilon=0.5$) and 33.1% ($Re=2.7x10^4$ and $\varepsilon=0$), whereas for average Nusselt numbers of human source are among 2.9% ($Re=2.7x10^3$ and $\varepsilon=0$) and 44.1% ($Re=2.7x10^3$ and $\varepsilon=0$). However the comparison between configurations (A) and (C), indicates that the percentage differences of average Nusselt numbers of heated wall are within -15.2% ($Re=2.0x10^4$ and $\varepsilon=0.5$) and 5.7% ($Re=2.7x10^3$ and $\varepsilon=0.5$), while for average Nusselt numbers of human source are among -27.1% ($Re=2.0x10^4$ and $\varepsilon=0.5$) and 4.2% ($Re=2.7x10^3$ and $\varepsilon=1$). Thus, configuration (B) produces the lower heat transfer from the heated wall and heat source.

The temperature distribution effectiveness for the studied cases is shown in Figure **5**. From this figure, it can be seen that configuration (A) presents the higher effectiveness indexes in most of the cases (except for $\varepsilon=0.5$ and air inlet velocities between 0.5m/s and 1.0m/s where configuration C is better). However, the highest effectiveness indexes are obtained for inlet between 0.2m/s and 1.0m/s, for higher values of inlet velocity effectiveness gradually decreases to an almost constant value. This result indicates that the best values for inlet velocities are between 0.2 and 1.0m/s because higher values for inlet velocity only increase energy consumption but do not improve temperature distribution effectiveness.

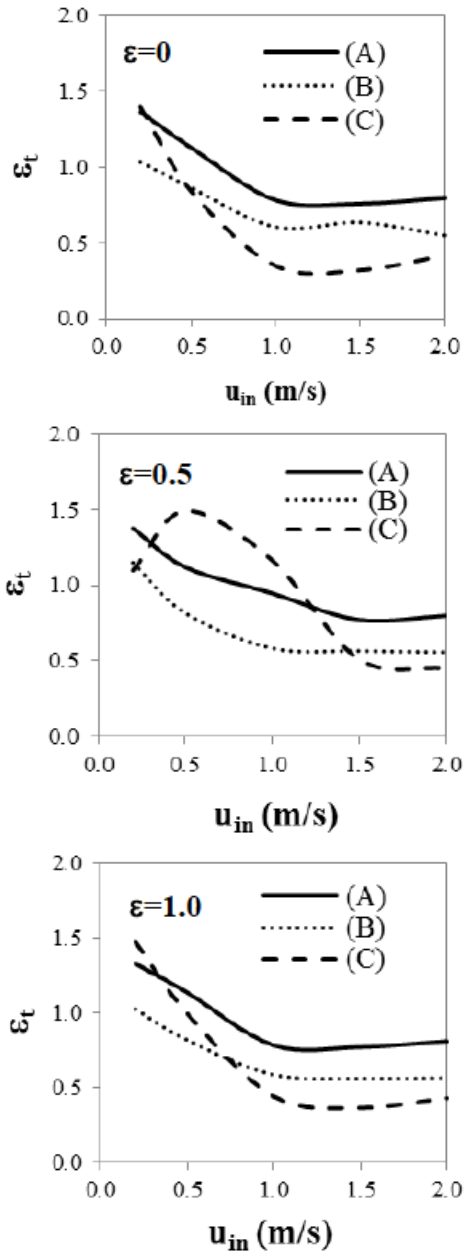

Figure 5: Temperature distribution effectiveness.

In Table **6**, the average temperatures together with its standard deviation for the considered cases are shown. It can be seen that increasing the air inlet velocity reduces the mean temperature inside the cavity, but for most of the cases it increases when is increased the emissivity of the walls. On the other hand ASHRAE Standard 55 [27] states that the temperatures for human comfort are between 22.7°C and 27.7°C, therefore the computed average temperatures are outside the comfort interval. Furthermore, it is observed that configuration (A) presents the lower average temperature inside the cavity and besides present's lower values for standard deviation so temperatures inside the cavity deviate less from average temperature.

Table 6: Average Temperatures (°C) with Standard Deviation inside the Ventilated Cavity

		u_{in} (m/s)	Re	ε=0	ε=0.5	ε=1
Configuration	A	0.2	$2.7x10^3$	20.0±3.0	20.3±3.5	20.9±3.2
		0.5	$6.7x10^3$	18.2±2.2	18.9±2.6	18.9±2.5
		1.0	$1.3x10^4$	18.3±1.9	18.0±2.5	19.0±2.1
		1.5	$2.0x10^4$	18.1±1.9	18.6±2.0	18.6±2.0
		2.0	$2.7x10^4$	17.8±1.7	18.2±1.8	18.3±1.7
	B	0.2	$2.7x10^3$	21.3±1.6	21.0±2.0	22.0±1.8
		0.5	$6.7x10^3$	18.7±2.1	19.9±2.3	20.1±2.3
		1.0	$1.3x10^4$	18.9±2.7	19.6±3.0	19.8±3.0
		1.5	$2.0x10^4$	18.1±2.1	19.1±2.8	19.3±2.8
		2.0	$2.7x10^4$	18.3±2.5	18.7±2.6	18.9±2.6
	C	0.2	$2.7x10^3$	19.9±2.8	21.1±4.2	20.8±2.9
		0.5	$6.7x10^3$	19.0±2.5	18.0±2.1	19.5±2.7
		1.0	$1.3x10^4$	20.5±3.1	17.4±1.8	20.9±3.3
		1.5	$2.0x10^4$	20.2±3.5	18.9±3.0	20.8±3.6
		2.0	$2.7x10^4$	19.0±2.6	19.3±2.5	19.9±3.0

Table 7: Velocity Magnitudes at Head and Shoulders (m/s) for Configuration (A)

u_{in} (m/s)	Re	ε=0		ε=0.5		ε=1	
		V_h	V_s	V_h	V_s	V_h	V_s
0.2	$2.7x10^3$	0.07	0.05	0.04	0.03	0.05	0.04
0.5	$6.7x10^3$	0.13	0.11	0.12	0.12	0.13	0.12
1.0	$1.3x10^4$	0.24	0.24	0.18	0.18	0.23	0.23
1.5	$2.0x10^4$	0.39	0.44	0.42	0.46	0.38	0.43
2.0	$2.7x10^4$	0.50	0.57	0.52	0.60	0.49	0.56

However according to the ASHRAE standard 55 [27] an air velocity value of 0.25m/s for the summer season is required. This criterion is based on experimental studies carried out on people submitted to an air flow 30cm away from their face and the back of the neck; thus velocity magnitudes smaller than 0.25m/s must be found at head and shoulders height. In Table **7** are presented velocity magnitudes at head (V_h) and shoulders (V_s) height in the ventilated cavity for configuration (A) which, according to previous results is the best option for the studied cavity. It is observed that, for the three emissivity values, 1.0m/s is the maximum permissible inlet velocity in order to assure the recommended velocity.

CONCLUSIONS

In this work is presented the numerical analysis of comfort conditions and heat transfer by natural and forced convection with thermal radiation, in an air-cooled ventilated two-dimensional cavity with a human heat source. Based on obtained results, the conclusions are:

1. The average total Nusselt numbers of heated wall and heat source increase substantially with the Reynolds number (inlet velocity) and the emissivity of the walls, however configuration (B) produces the lower heat transfer.

2. The configuration (A) presents higher temperature distribution effectiveness (except for ε=0.5 and air inlet velocities between 0.5m/s and 1.0m/s where configuration C is better).

3. The better values of inlet velocity are between 0.2 and 1.0m/s because higher values for velocity only increase energy consumption but do not improve temperature distribution effectiveeness.

4. Increasing the air inlet velocity reduces the mean temperature inside the cavity with configuration (A) presenting the lower average temperature inside the cavity.

5. For the three emissivity values, 1.0m/s is the maximum permissible inlet velocity in order to

assure the recommended velocity by ASHRAE standard 55 for comfort conditions.

REFERENCES

[1] Raji A and Hasnaoui M. Mixed convection heat transfer in a rectangular cavity ventilated and heated from the side. Numerical Heat Transfer Part A 1998; 33: 533-548. http://dx.doi.org/10.1080/10407789808913953

[2] Raji A and Hasnaoui M. Mixed convection heat transfer in ventilated cavities with opposing and assisting flows. Engineering Computations 2000; 17: 556-572. http://dx.doi.org/10.1108/02644400010339770

[3] Raji A and Hasnaoui M. Combined mixed convection and radiation in ventilated cavities. Engineering Computations 2001; 18: 922-949. http://dx.doi.org/10.1108/EUM0000000006212

[4] Singh S and Sharif MAR. Mixed convective cooling of a rectangular cavity with inlet and exit openings on differentially heated side walls. Numerical Heat Transfer Part A 2003; 44: 233-253. http://dx.doi.org/10.1080/716100509

[5] Posner J. Measurement and prediction of indoor air flow in a model room. Energy and buildings 2003; 35: 515-526. http://dx.doi.org/10.1016/S0378-7788(02)00163-9

[6] Moraga NO and Lopez SE. Numerical simulation of three-dimensional mixed convection in an air-cooled cavity. Numerical Heat Transfer Part A: Applications 2004; 45: 811-824. http://dx.doi.org/10.1080/10407780490250409

[7] Haslavsky V, Tanny J and Teitel M. Interaction between the mixing and displacement modes in a naturally ventilated enclosure. Building and Environment 2006; 41: 1755-1761. http://dx.doi.org/10.1016/j.buildenv.2005.07.013

[8] Rahman M, Alim M, Mamun M, Chowdhury MK and Islam AKMS. Numerical study of opposing mixed convection in a vented enclosure. ARPN J Eng and Appl Sciences 2007; 2: 25-36.

[9] Daghigh R, Adam N, Sahari B, Sopian K and Alghoul M. Influences of air exchange effectiveness and its rate on thermal comfort: Naturally ventilated office. Journal of Building Physics 2008; 32: 1744-2591. http://dx.doi.org/10.1177/1744259108097333

[10] Raji A, Hasnaoui M and Bahlaoui A. Numerical study of natural convection dominated heat transfer in a ventilated cavity case of force flow playing simultaneous assisting and opposing roles. International Journal of Heat and Fluid Flow 2008; 29: 1174-1181. http://dx.doi.org/10.1016/j.ijheatfluidflow.2008.01.010

[11] Saha S, Mamun A, Hossain Z and Islam S. Mixed convection in an enclosure with different inlet and exit configurations. Journal of Applied Fluid Mechanics 2008; 1: 78-93.

[12] Tanny J, Haslavsky V and Teitel M. Airflow and heat flux through the vertical opening of buoyancy-induced naturally ventilated enclosures. Energy and Buildings 2008; 40: 637-646. http://dx.doi.org/10.1016/j.enbuild.2007.04.020

[13] Lariani A, Nesreddine H and Galanis N. Numerical and experimental study of 3D turbulent airflow in a full scale heated ventilated room. Engineering Applications of Computational Fluid Mechanics 2009; 3: 1-14. http://dx.doi.org/10.1080/19942060.2009.11015250

[14] Xamán J, Tun J, Álvarez G, et al. Optimum ventilation based on the overall ventilation effectiveness for temperature distribution in ventilated cavities. International Journal of Thermal Sciences 2009; 48: 1574-1585. http://dx.doi.org/10.1016/j.ijthermalsci.2008.12.008

[15] Rodriguez NA and Hinojosa JF. Numerical study of airflow and heat transfer in an air-cooled room with different inlet positions. Journal of Building Physics 2014; 37: 246-268. http://dx.doi.org/10.1177/1744259112462106

[16] Papanicolaou E and Jaluria Y. Mixed convection from an isolated heat source in a rectangular enclosure. Numerical Heat Transfer Part A 1990; 18: 427-461. http://dx.doi.org/10.1080/10407789008944802

[17] Papanicolaou E and Jaluria Y. Mixed convection from localized heat source in a cavity with conducting walls. Numerical Heat Transfer Part A 1993; 23: 463-484. http://dx.doi.org/10.1080/10407789308913683

[18] Hsu T and Wang S. Mixed convection in a rectangular enclosure with discrete heat sources. Numerical Heat Transfer Part A 2000; 38: 627-652. http://dx.doi.org/10.1080/104077800750021170

[19] Radhakrishnan T, Verma A, Balaji C, et al. An experimental and numerical investigation of mixed convection from a heat generating element in a ventilated cavity. Experimental Thermal and Fluid Science 2007; 32: 502-520. http://dx.doi.org/10.1016/j.expthermflusci.2007.06.001

[20] Ghasemi B and Aminossadati SM. Numerical simulation of mixed convection in a rectangular enclosure with different numbers and arrangements of discrete heat sources. The Arabian Journal for Science and Engineering 2008; 33: 189-207.

[21] Bilgen E and Muftuoglu A. Cooling strategy by mixed convection of a discrete heater at its optimum position in a square cavity with ventilation ports. Int. Comm. in Heat and Mass Transfer 2008; 35: 545-550. http://dx.doi.org/10.1016/j.icheatmasstransfer.2008.01.001

[22] Villase-or-Mora C, Sanchez-Marin FJ and Calixto-Carrera S. An indirect skin emissivity measurement in the infrared thermal range through reflection of a CO2 laser beam. Revista Mexicana de Fisica 2009; 55: 387-392.

[23] Ince N and Launder B. On the computation of buoyancy driven turbulent flows in rectangular enclosures. International Journal of Heat and Fluid Flow 1989; 10: 110-117. http://dx.doi.org/10.1016/0142-727X(89)90003-9

[24] Nielsen P. Specification of a two dimensional test case, Energy Conservation in Buildings and Community System. Annex 20 (1990).

[25] Awbi H. Ventilation of buildings. E and FN Spon (2003).

[26] Patankar S. Numerical Heat Transfer and Fluid Flow. Hemisphere Publishing, Washington (1980).

[27] ASHRAE Standard 55. Thermal environment conditions for human occupancy (2004).

Received on 14-12-2015 Accepted on 01-01-2016 Published on 13-07-2016

DOI: http://dx.doi.org/10.15377/2409-5826.2016.03.01.1